Biochimica et Biophysica Acta 1827 (2013) 861–868

Contents lists available at SciVerse ScienceDirect

Biochimica et Biophysica Acta

journal homepage: www.elsevier.com/locate/bbabio

Thermodynamically accurate modeling of the catalytic cycle of photosynthetic oxygen evolution: A mathematical solution to asymmetric Markov chains

David J. Vinyard [a,b,c], Chase E. Zachary [c], Gennady Ananyev [a,b], G. Charles Dismukes [a,b,*]

[a] Department of Chemistry and Chemical Biology, Rutgers, The State University of New Jersey, Piscataway, NJ 08854, USA
[b] Waksman Institute of Microbiology, Rutgers, The State University of New Jersey, Piscataway, NJ 08854, USA
[c] Department of Chemistry, Princeton University, Princeton, NJ 08540, USA

ARTICLE INFO

Article history:
Received 6 March 2013
Received in revised form 19 April 2013
Accepted 23 April 2013
Available online 30 April 2013

Keywords:
Photosystem II
Photosynthetic efficiency
Oxygen evolution
Markov chain
Kok model

ABSTRACT

Forty-three years ago, Kok and coworkers introduced a phenomenological model describing period-four oscillations in O_2 flash yields during photosynthetic water oxidation (WOC), which had been first reported by Joliot and coworkers. The original two-parameter Kok model was subsequently extended in its level of complexity to better simulate diverse data sets, including intact cells and isolated PSII-WOCs, but at the expense of introducing physically unrealistic assumptions necessary to enable numerical solutions. To date, analytical solutions have been found only for symmetric Kok models (inefficiencies are equally probable for all intermediates, called "S-states"). However, it is widely accepted that S-state reaction steps are not identical and some are not reversible (by thermodynamic restraints) thereby causing asymmetric cycles. We have developed a mathematically more rigorous foundation that eliminates unphysical assumptions known to be in conflict with experiments and adopts a new experimental constraint on solutions. This new algorithm termed STEAMM for S-state Transition Eigenvalues of Asymmetric Markov Models enables solutions to models having fewer adjustable parameters and uses automated fitting to experimental data sets, yielding higher accuracy and precision than the classic Kok or extended Kok models. This new tool provides a general mathematical framework for analyzing damped oscillations arising from any cycle period using any appropriate Markov model, regardless of symmetry. We illustrate applications of STEAMM that better describe the intrinsic inefficiencies for photon-to-charge conversion within PSII-WOCs that are responsible for damped period-four and period-two oscillations of flash O_2 yields across diverse species, while using simpler Markov models free from unrealistic assumptions.

1. Introduction

In oxygenic photosynthesis, water is oxidized by the Photosystem II (PSII) water-plastoquinone (PQ) oxidoreductase. Following the absorption of visible light, charge separation occurs at the P_{680} chlorophyll-*a* (Chl-a) special pair, resulting in the sequential one-electron transfers to pheophytin (Pheo), the tightly bound (primary) PQ acceptor, Q_A, and the labile (secondary) PQ acceptor, Q_B. The latter reduction is proton-coupled and occurs twice to form plastoquinol $(PQH_2)_B$, which diffuses from the binding pocket and is replaced with an oxidized PQ [1,2]. The remaining P_{680}^+ species has sufficient oxidizing potential (1.2–1.3 V [3]) to remove one electron from the Mn_4CaO_5 water-oxidizing complex (WOC) via a conserved redox active tyrosine residue, D1-Tyr161 (Y_Z). Following four sequential charge separations and WOC oxidations, two molecules of water are oxidized to form one molecule of O_2 and two molecules of PQH_2 (Eq. 1).

$$2H_2O + 2PQ + 4h\nu \rightarrow O_2 + 2PQH_2 \tag{1}$$

When short (ns–μs scale) flashes of light are used to excite dark-adapted PSII, O_2 is released in greatest yield on the third flash and follows a damped period-four oscillatory pattern [4]. To rationalize this observation, Kok and coworkers posited a mechanism in which each PSII operated independently to accumulate four electron holes in a single redox center (WOC catalyst) [5,6]. The intermediate oxidation states of the PSII WOC were denoted S_n ($n = 0, 1, 2, 3, 4$). The S_0 and S_1 state were described as dark stable, thus allowing samples to be synchronized through several minutes of dark adaptation. Three sequential single turnover flashes advance the centers from S_1 (S_0) to S_4 (S_3). Only the S_4 state spontaneously decomposes to release O_2 and form S_0 (Fig. 1). In an ideal Kok system, O_2 is released on flash numbers $3 + 4n$ ($n = 0, 1, 2, \ldots$).

---

[*] Corresponding author at: Waksman Institute of Microbiology, Rutgers, The State University of New Jersey, 190 Frelinghuysen Rd., Piscataway, NJ 08854, USA. Tel.: +1 848 445 6786; fax: +1 732 445 5735.
E-mail address: dismukes@rci.rutgers.edu (G.C. Dismukes).

0005-2728/$ – see front matter © 2013 Elsevier B.V. All rights reserved.
http://dx.doi.org/10.1016/j.bbabio.2013.04.008

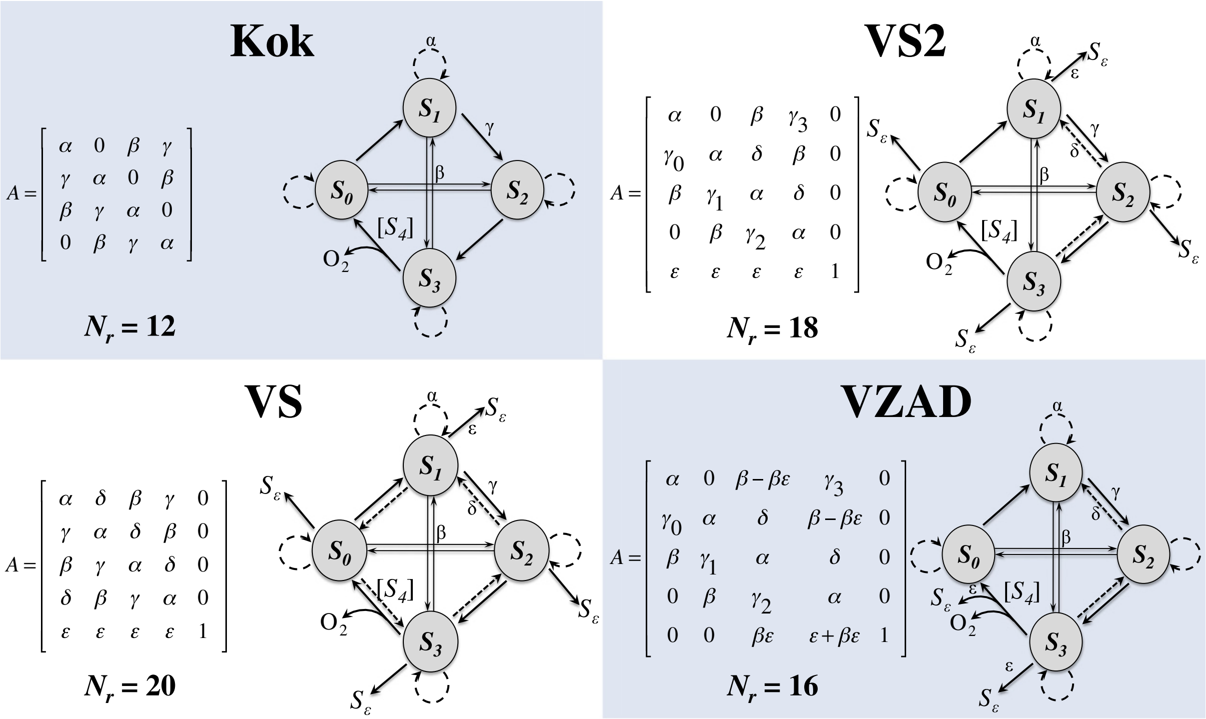

Fig. 1. Transition probability matrices and graphical models for the models studied in this work. N_r represents the number of distinct reactions in each model.

The damping of the oscillations in O_2 evolution in real systems is attributed to inefficiencies of PSII in the water oxidation cycle (period-four) [5] and to restricted flux through Q_AQ_B (the two-electron gate) [7]. Jablonsky and Lazar have successfully modeled this phenomenon using experimental and theoretical rate constants of intermediate S-state transitions [8]. In addition, the sharing of holes between individual reaction centers within the dimeric PSII complex has been postulated to give rise to O_2 on the second flash, prior to accumulation of four holes per individual PSII [9]. This could lead to deviations from the period-four oscillations indicative of isolated reaction centers. The classic Kok model quantifies the inefficiencies with two empirical parameters: misses (α: $S_n + h\nu \rightarrow S_n$) and double hits ($\beta$: $S_n + h\nu \rightarrow S_{n+2}$) [5]. By recognizing that the Kok model is a Markov process (i.e. a stochastic, memory-less sequence), experimental data of all kinds have been readily fit by iterative (recursive) mathematical algorithms [10,11]. Prior applications of the Kok model have included period-four oscillations in chlorophyll absorbance [12,13], proton stoichiometry and kinetics [14,15], chlorophyll fluorescence [16,17], Mn electron paramagnetic resonance signal [18], Mn ultraviolet absorbance [19,20], magnetic susceptibility [21], and substrate water exchange rates [22], among others.

The classic Kok model has been extended since its inception to improve fits to experimental data. These extensions have included additional S-states to represent the spectroscopically observed S_{-1} state [23] and an inactivated state S_ε (accessed with probability ε) [24]. A backward transition parameter, δ, was introduced to account for the spontaneous decay of S_3 and S_2 [25].

Shinkarev first introduced an analytical solution to the classic Kok model [26]. Later, he developed an analytical solution to an extended Kok model that included the S_ε state (accessed with equal probability from all S-states) and δ parameters for all S_n ($n = 0, 1, 2, 3$) [27]. The mathematical methods employed in both of these solutions are facilitated by circulant transition probability matrices, making eigenvalues and eigenvectors readily accessible [28]. The availability of an analytical solution permits standard regression methods to be used to fit experimental data.

The efficiency of WOC cycling can be assessed without modeling by taking the Fourier transform (FT) of the oscillatory trace. The real component of the FT function is an approximate Gaussian function centered at frequency, $\nu > 0.25$ cycles^{-1}. The FT period, T_{FT}, is defined as the inverse of the frequency value with maximum Fourier amplitude. T_{FT} can readily be related to the phase of the original function, φ_{FT}, as shown in Eq. 2.

$$T_{FT} = 1/\nu = 2\pi/\varphi_{FT} \tag{2}$$

This model-independent parameter has been used to quantify the efficiency of WOC cycling in flash O_2 evolution [29] and variable Chl-a fluorescence yield [29–33].

If the eigenvalues of a specific Kok model's transition probability matrix are known, period and phase can be calculated (denoted herein as T_{calc} and φ_{calc}, respectively) as a function of the fitted inefficiency parameters (α, β, etc.) [26,27]. To date, this has only been possible for symmetric Kok models.

However, the current understanding of WOC thermodynamics and kinetics predicts that the natural system does not follow symmetric behavior. For example, only S_3 and S_2 undergo δ transitions [34,35]; S_1 and S_0 are dark stable. If the extended Shinkarev model [27] is amended to account for asymmetric δ transitions, the transition probability matrix is no longer circulant, and the mathematical methods previously employed are insufficient to arrive at an analytical solution and T_{calc}.

Herein, we introduce a novel application of matrix analysis methods that allows analytical solutions to be accessed from non-circulant, thermodynamically reasonable Kok models. We show that a diverse range of experimental data can be fit with good precision using fewer total parameters than previous fully extended models. In addition, our updated model predicts period with high accuracy when compared to model-independent Fourier transform analysis.

2. Materials and methods

Flash O_2 yields were measured amperometrically using a home-built Clark electrode (membrane-covered Pt–Ir electrode) as previously described [36]. A red LED (6,200 $\mu E\ m^{-2}\ s^{-1}$, $\lambda_{max} = 627$ nm) was used to generated flashes. Detailed experimental methods for all data sets are described in Supplementary data.

Data from Forbush et al. [5] on spinach chloroplasts were simulated using fitting parameters from Shinkarev [27]. *Arthrospira maxima* (*A. maxima*) was grown in Zarrouk medium as previously described [30]. *Gloeobacter violaceus* PCC 7421 (*G. violaceus*) was grown in BG-11 medium at 10 $\mu E\ m^{-2}\ s^{-1}$.

Full oscillating traces of flash O_2 yield were normalized to achieve a steady-state value of 0.25. Fittings were determined by minimizing an objective function proportional to the mean-square deviation from the experimental curve using either the BOBYQA [37] or COBYLA [38] algorithm in the NLopt non-linear optimization package [39], or through classical simulated annealing [40]. The goal of all of the methods employed is to minimize an objective function, J, defined as the square difference between a fitting function, $f(n)$ and experimental data, $f'(n)$:

$$J = \sum_n \left[f(n) - f'(n)\right]^2 \tag{3}$$

3. Results and discussion

3.1. Analytical determination of the transition eigenvalues for non-circulant Kok models

Consider a transition probability matrix A for a Kok model defined by a set of transition probabilities $\{A_{ij}\}$, where A_{ij} is the probability of transitioning to state S_i from state S_j following a single turnover flash. Note that conservation of matter requires

$$\sum_{i=1}^{N_S} A_{ij} = 1 \qquad for\ \ all\ \ j, \tag{4}$$

where N_S is the number of intermediates (S-states) in the model. For example, the transition probability matrix for the original Kok model [5] is given by

$$A = \begin{bmatrix} \alpha & 0 & \beta & \gamma \\ \gamma & \alpha & 0 & \beta \\ \beta & \gamma & \alpha & 0 \\ 0 & \beta & \gamma & \alpha \end{bmatrix}, \tag{5}$$

where $\alpha + \beta + \gamma = 1$, where γ is the "hit" parameter ($S_n + h\nu \rightarrow S_{n+1}$).

Following the analysis by Shinkarev [26], the vector $\mathbf{S}(n)$ of S-state populations after turnover flash n is

$$\mathbf{S}(n) = A^n \mathbf{S}(0) = P \Lambda^n P^{-1} \mathbf{S}(0), \tag{6}$$

where P is a matrix consisting of the eigenvectors of A [28], and Λ is a diagonal matrix with the eigenvalues of A providing the nonzero entries. In principle, Eq. 6 constitutes a complete solution to the Kok model for S-state transitions; however, the utility of this approach is limited by the ability to analytically determine the eigenvectors and eigenvalues of the transition matrix A. Of particular interest is the set of eigenvalues $\{\lambda_j\}$ of A, which generally includes one or more pairs of complex conjugate eigenvalues that are responsible for the signature oscillatory behavior of oxygen evolution following single turnover flashes [26,27]. Specifically, if the model contains a pair of complex conjugate eigenvalues, the period T of these oscillations is given by [26,27]

$$T_{calc} = 2\pi / \varphi_{calc} \tag{7}$$

where φ_{calc}, denoted the phase, is the argument of a complex eigenvalue $\lambda = u + iv$:

$$\varphi_{calc} = arccos\left(\frac{u}{\sqrt{u^2 + v^2}}\right). \tag{8}$$

The transition matrix A for the traditional Kok model is an example of a so-called circulant matrix, defined by [41]

$$A = \begin{bmatrix} a_0 & a_{N-1} & \cdots & a_1 \\ a_1 & a_0 & \cdots & a_2 \\ \vdots & \ddots & \ddots & \vdots \\ a_{N-1} & \cdots & \cdots & a_0 \end{bmatrix}. \tag{9}$$

The eigenvalues and eigenvectors of circulant matrices are well known (see, e.g., Ref. [42]). The eigenvectors $\{\mathbf{v}_j\}$ are given by

$$\mathbf{v}_j = \begin{bmatrix} 1 \\ \omega_j \\ \omega_j^{\,2} \\ \vdots \\ \omega_j^{\,N-1} \end{bmatrix}, \tag{10}$$

where $\omega_j = \exp(2\pi ij/N)$ is the Nth root of unity and i is the imaginary unit. The eigenvalues $\{\lambda_j\}$ of a circulant matrix are then given by

$$\lambda_j = \left(\mathbf{A}_1,\ \mathbf{v}_j\right)_R, \tag{11}$$

where $\mathbf{A}_1$ is the vector formed from the first row of the circulant matrix A and $(\cdot,\cdot)_R$ denotes the dot product between two complex d-dimensional vectors:

$$(\mathbf{a},\ \mathbf{b})_R = \sum_{j=1}^{d} a_j b_j. \tag{12}$$

Because the eigenvectors and eigenvalues for the traditional and extended Kok models studied previously by Shinkarev [26,27] are readily available, analytical solutions for these models, including the periods of oscillations, are straightforward. Here we extend the Shinkarev analysis to more complex Kok models with transition matrices that are non-circulant, which until now has precluded an analytical determination of the eigenvalues and eigenvectors.

Decompose the transition matrix A into the sum of a circulant matrix A_0 and a non-circulant "perturbation" matrix E:

$$A = A_0 + E. \tag{13}$$

The eigenvalues $\{\lambda_j\}$ and eigenvectors $\{\mathbf{v}_j\}$ of A_0 are known from Eqs. 10–11 above. Importantly, the eigenvectors of A_0 are linearly independent and orthogonal and therefore span complex N_S-dimensional space, implying that any eigenvector $\boldsymbol{\eta}$ of A can be written as a linear combination of the eigenvectors of A_0:

$$\boldsymbol{\eta} = \sum_j b_j \mathbf{v}_j, \tag{14}$$

where b_j is an undetermined expansion coefficient. The eigenvalue ρ corresponding to the eigenvector $\boldsymbol{\eta}$ is by definition,

$$\begin{aligned} &A\boldsymbol{\eta} = \rho\boldsymbol{\eta} = \sum_j b_j (A_0 + E)\mathbf{v}_j \\ &\Rightarrow \rho \sum_j b_j \mathbf{v}_j = \sum_j b_j \left(\lambda_j I + E\right)\mathbf{v}_j \\ &\Rightarrow \sum_j b_j \left[\left(\lambda_j - \rho\right) I + E\right]\mathbf{v}_j = \mathbf{0}. \end{aligned} \tag{15}$$

Taking the inner product of both sides of Eq. 15 with another eigenvector $\mathbf{v}_k$ of A_0 yields the following set of nonlinear equations in the unknowns $\{b_j; \rho\}$:

$$b_k(\mathbf{v}_k, \mathbf{v}_k)(\lambda_k - \rho) + \sum_j b_j \left(\mathbf{v}_k, E\mathbf{v}_j\right) = 0, \tag{16}$$

where

$$(\mathbf{c}, \mathbf{d}) = \sum_j \overline{c_j} d_j \tag{17}$$

is the Euclidean inner product of two complex vectors $\mathbf{c}$ and $\mathbf{d}$. The set of Eqs. 14–17 is only weakly nonlinear with coupling between b_k and ρ and can be solved analytically for many models for which the characteristic equation for A is otherwise intractable. Note in particular that we can without loss of generality set $b_k = 1$ for some choice of k, thereby reducing the number of unknown variables from $N_S + 1$ to N_S, permitting a complete determination of both the eigenvalues and eigenvectors of the full transition matrix A. As expected, the eigenvalues ρ will generally be small perturbations of the circulant eigenvalues $\{\lambda_j\}$ based on the spectrum of the perturbation matrix E. However, the eigenvectors $\boldsymbol{\eta}$ of A will generally involve substantial mixing of the circulant eigenvectors $\{\mathbf{v}_j\}$ even when the spectral radius of E is not large [41].

If, however, we are only interested in finding the eigenvalues ρ, which can be used for analytical determinations of the period of experimental oscillations, of the transition matrix A, yet another approach is available that circumvents calculation of the coefficients. Defining the vector $\mathbf{b} = [b_k]$ and the matrices $E_1 = [(\mathbf{v}_k, E\mathbf{v}_j)]$ and $D(\rho) = \mathrm{diag}[(\mathbf{v}_k, \mathbf{v}_k)(\lambda_k - \rho)]$, the Eq. 16 can be rewritten as

$$[E_1 + D(\rho)]\mathrm{b} = \mathbf{0}. \tag{18}$$

It is then a necessary and sufficient condition for a nontrivial solution of Eq. 18 to exist that

$$\det[E_1 + D(\rho)] = 0, \tag{19}$$

which is a polynomial equation in the eigenvalues ρ [28]. Although in principle this polynomial is of the same order as the characteristic equation for A, our calculations suggest that the solution of Eq. 19 may be computationally less intensive for many models.

3.2. Numeric solutions for non-circulant Kok models

Consider the transition probability matrix, A, of the VS2 model shown in Fig. 1, which differs in only two elements from the extended Shinkarev (VS) model.

Removal of the δ parameter for the $S_0 \rightarrow S_3$ and $S_1 \rightarrow S_0$ better reflects the thermodynamics of WOC cycling, but breaks the symmetry of the model. In order to determine an analytical solution for this model, we introduce a novel mathematical method termed STEAMM for S-state Transition Eigenvalues of Asymmetric Markov Models. Note that for asymmetric Kok models, γ is not constant. Conservation of matter dictates that $\gamma_0 = \gamma_1 = 1 - \alpha - \beta - \varepsilon$ and $\gamma_2 = \gamma_3 = 1 - \alpha - \beta - \delta - \varepsilon$. However, by applying the approach described in the previous section, matrix A representing VS2 can be decomposed into

$$A = \begin{bmatrix} \alpha & \delta & \beta & \gamma_3 & 0 \\ \gamma_0 & \alpha & \delta & \beta & 0 \\ \beta & \gamma_1 & \alpha & \delta & 0 \\ \delta & \beta & \gamma_2 & \alpha & 0 \\ \varepsilon & \varepsilon & \varepsilon & \varepsilon & 1 \end{bmatrix} + \begin{bmatrix} 0 & -\delta & 0 & 0 & 0 \\ 0 & 0 & 0 & 0 & 0 \\ 0 & 0 & 0 & 0 & 0 \\ -\delta & 0 & 0 & 0 & 0 \\ 0 & 0 & 0 & 0 & 0 \end{bmatrix} \tag{20}$$

The eigenvalues can now be readily accessed using Eq. 19.

$$\begin{aligned} &\rho_1 = 1 \\ &\rho_2 = 1 - \varepsilon \\ &\rho_3 = 2(\alpha + \beta) - 1 + \varepsilon \\ &\rho_4 = (\alpha - \beta) - i(1 - \alpha - \beta - \delta - \varepsilon) \\ &\rho_5 = (\alpha - \beta) + i(1 - \alpha - \beta - \delta - \varepsilon) \end{aligned} \tag{21}$$

Thus, the phase of the model is

$$\varphi_{\mathrm{calc}} = \arccos\left(\frac{\alpha - \beta}{\sqrt{(\alpha - \beta)^2 + (1 - \alpha - \beta - \delta - \varepsilon)^2}}\right) \tag{22}$$

The population passing through the $S_3 \rightarrow S_0$ transition on a given flash number n determines the yield of O_2 evolution (Y_{O_2}):

$$Y_{O_2}(n) = (\gamma + \beta)[S_3](n - 1) + \beta[S_2](n - 1) \tag{23}$$

An extension of this method to a more complex model is provided in Appendix A.

3.3. Comparison of non-linear optimization methods

Data from Forbush et al. [5] were numerically fit using STEAMM to the VZAD model (Eqs. 23–27) using three distinct non-linear optimization algorithms: BOBYQA [37], COBYLA [38], and simulated annealing [40]. While the computing time varied significantly between the three methods (<1 s for BOBYQA, ~3 s for COBYLA, and 490 s for simulated annealing), the fitted data (Fig. 2) and parameters (Table S1) were identical to three significant figures. Given the high degree of agreement between the methods, BOBYQA was used for all further analyses due to its rapid process time.

3.4. Data fittings to symmetric and asymmetric Kok models

Three distinct data sets from diverse organisms were selected for comparisons of symmetric and asymmetric Kok models. First, the original data of flash O_2 oscillations from isolated spinach chloroplasts measured using a bare platinum electrode by Forbush et al. [5] were fit to the classic Kok model, extended Shinkarev 2005 [27] (VS), reduced Shinkarev (VS2), and VZAD. As shown in Fig. 3, all four models provide reasonably precise fits. The simple Kok model is least precise (largest residuals (Fig. 3A) and largest minimized energy (Eq. 3, Fig. 3B and Table S2)). As expected, the classic Kok model does not capture the small amplitude oscillations of period-two (see residuals plot in Fig. 3A), attributable to either the different electron fluxes through or recombination from Q_AQ_B [7], or to hole transfer on the donor side between reaction center monomers within dimeric

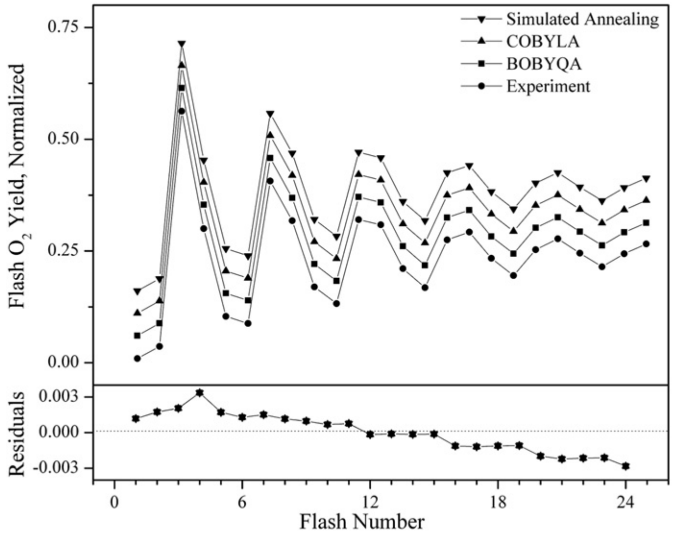

Fig. 2. Fitting of flash O_2 evolution data from isolated spinach chloroplasts digitized from Forbush et al. (1971) using the VZAD model and various non-linear optimization methods. Data in upper panel are offset for clarity. Full fitting data are shown in Table S1. Experimental conditions are summarized in Table S1 legend.

PSII complexes [9]. The remaining three models result in practically identical degrees of fitting precision. The accuracy of the fits was analyzed by comparing the calculated period, T_{calc} (e.g. Eqs. 7–8 for the classic Kok model), to the readily accessible Fourier transform period, T_{FT} (Eq. 2). As shown in Fig. 3B, VS, VS2, and VZAD models produce significantly more accurate fittings of the experimental data than the classic Kok model.

Next, we considered whole *A. maxima* cells as they produce maximal O_2 yield over the widest flash frequency range of any oxygenic phototroph [30]. Here, the use of whole cells and a membrane covered (Clark) electrode introduces diffusion delays relative to the isolated chloroplast data recorded on a bare platinum electrode (Figs. 1–2). Oscillations in O_2 yield from *A. maxima* cells were analyzed using the same set of models (Fig. 4A). Again, the classic Kok model failed to fit the data with high precision or accuracy (Fig. 4B, Table S3). The residuals are similar over 30 flashes for all of the models, indicating that none of the models fully captures all of the reaction details, in particular, the small amplitude oscillations of period-two from flash 20 to 30 (see residuals plots in Fig. 4A), attributable to the different electron fluxes through or recombination from Q_AQ_B [7] or to hole transfer on the donor side between reaction center monomers within dimeric PSII complexes [9].

To challenge our STEAMM method, we next fitted highly damped oscillations from whole *G. violaceus* cells, which unlike the previous examples has peak O_2 evolution on flash number 4, not 3. *G. violaceus* is the only known oxygenic phototroph in which photosynthetic and respiratory complexes are located in the plasma membrane, thus coupling plastoquinone reduction by PSII with other reductant pathways [43]. The classic Kok model could not satisfactorily fit the experimental data as demonstrated by visual inspection (Fig. 5A) and the large calculated accuracy and precision parameters (Fig. 5B and Table S4). Both the VS2 and VZAD models performed slightly better in terms of accuracy than VS.

3.5. Dependence of number of variables on fitting accuracy and precision

The transition probability matrices, *A*, for Kok, VS, VS2, and VZAD models (Fig. 1) vary significantly in their complexity as defined by N_{r}, the number of distinct reactions per model. The VS model ($N_{\mathrm{r}} = 20$) is vastly superior to the Kok model ($N_{\mathrm{r}} = 12$) in terms of fitting data with high accuracy and precision (Figs. 3–5). Interestingly, when unreasonable backward (δ) transitions are removed to generate the VS2 model ($N_{\mathrm{r}} = 18$), no significant loss in accuracy or precision is observed. Furthermore, when inactivation (ε) transitions that are universally applied to all S-states in the latter models are reduced to generate the VZAD model ($N_{\mathrm{r}} = 16$), fits are quite comparable to both VS and VS2.

We propose that the fully symmetric VS model is overdeveloped in its level of complexity. By systematically reducing the number of elements in *A* based on known PSII WOC chemistry, we have generated simpler models that fit data with high accuracy and precision using fewer variables.

4. Conclusions

Herein, we have described a general mathematical strategy for obtaining the eigenvalues of asymmetric Markov chains and applied this to physically realistic "Kok models." Using the STEAMM method, experimental data can be analytically fit and resulting accuracy and precision quantified. No study on the modeling of period-four

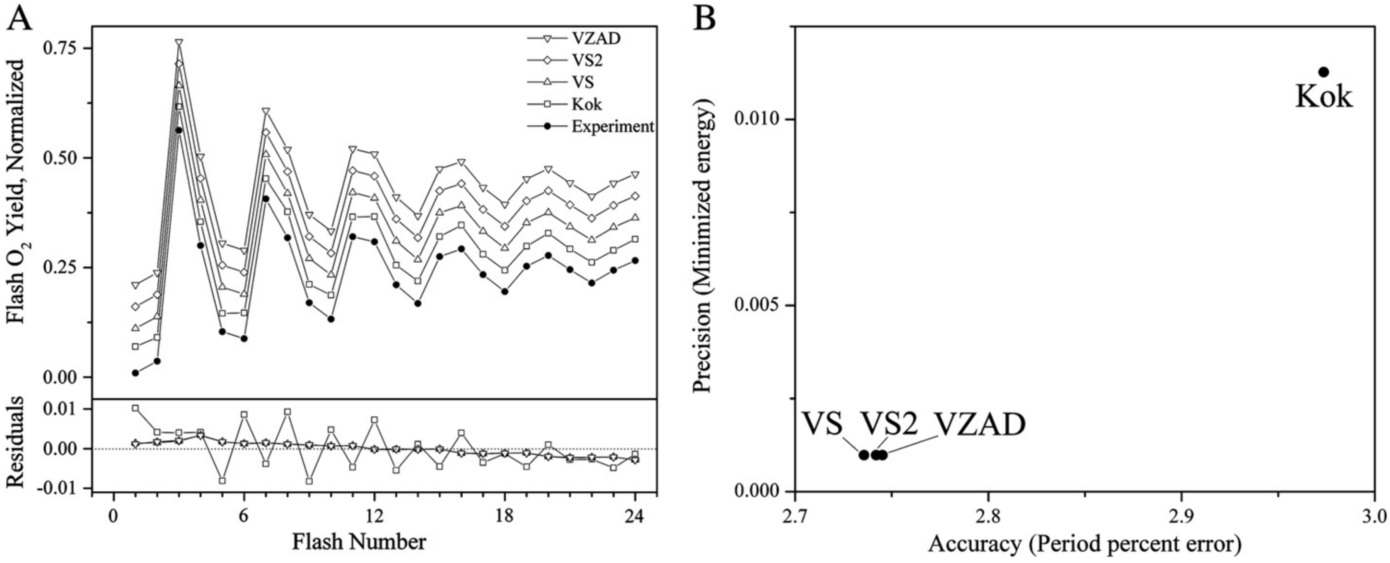

Fig. 3. (A) Fitting of flash O_2 evolution data from isolated spinach chloroplasts digitized from Forbush et al. (1971) using the models shown in Fig. 1. Data are offset for clarity. (B) Comparisons of accuracy and precision for the resulting fits. Full fitting data are shown in Table S2. Experimental conditions are summarized in Table S1 legend.

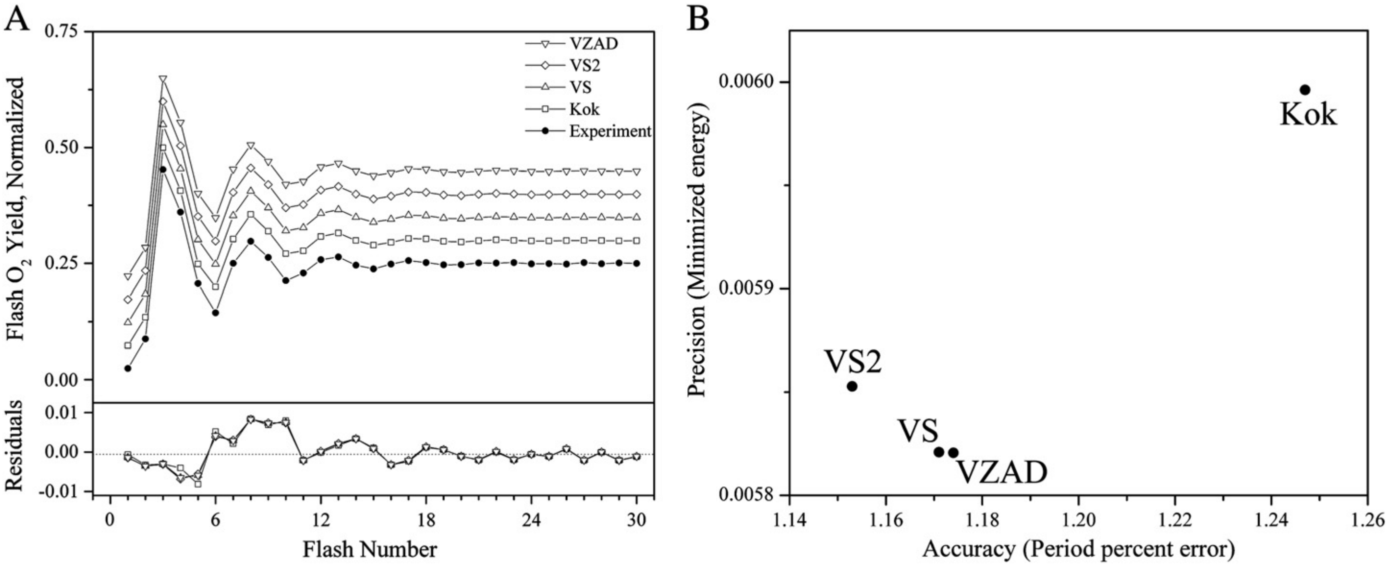

Fig. 4. (A) Fitting of flash O_2 evolution data from whole *A. maxima* cells using the models shown in Fig. 1. Data are offset for clarity. (B) Comparisons of accuracy and precision for the resulting fits. Full fitting data are shown in Table S3. Experimental conditions are summarized in Table S3 legend.

oscillations in photosynthetic water oxidation to date has considered the accuracy index (comparison of T_{calc} to T_{FT}) of various Kok models. With this method and data in hand, we show that the classic Kok model is insufficient to fit experimental data in terms of both accuracy and precision. While symmetrical models such as VS often provide adequate fits, the inclusion of transition probability matrix elements that are known to be thermodynamically unreasonable excludes such models from being directly applicable to real systems. The asymmetric models VS2 and VZAD both fit the diverse data shown here with good accuracy and precision, even though they contain fewer variables than VS.

The models and data sets chosen for this study illustrate the utility of the STEAMM method, but are by no means all-inclusive. Instead, STEAMM provides a uniform mathematical groundwork for analyzing damped oscillations of any periodicity using any appropriate Markov model, regardless of symmetry. With this more powerful toolbox, it is now possible to analyze with greater confidence reaction models that extend the physical meaning of oscillations.

Acknowledgements

This work was funded by the Division of Chemical Sciences, Geosciences, and Biosciences, Office of Basic Energy Sciences of the U.S. Department of Energy (Grant DE-FG02-10ER16195). D.J.V. is supported by the Department of Defense, Army Research Office through a National Defense Science and Engineering Graduate (NDSEG) Fellowship, 32CFR168a, and a National Science Foundation Graduate Research Fellowship, DGE-0937373.

Appendix A

We may extend the approach used for the VS2 model (Eqs. 20–23) to a more complex model in which only thermodynamically reasonable δ transitions are allowed (like VS2) and ε is linked to selected states, specifically the O_2-releasing step. We hypothesize that reactive oxygen species generated in the $S_3 \rightarrow S_0$ transition are selectively

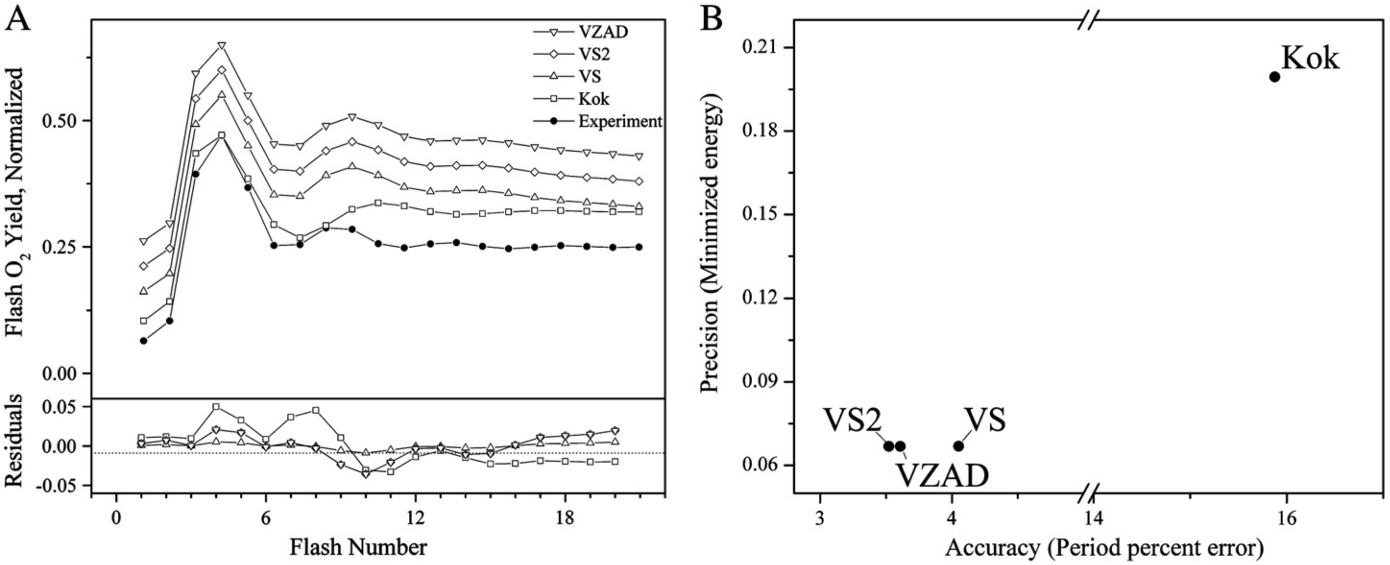

Fig. 5. (A) Fitting of flash O_2 evolution data from whole *G. violaceus* cells using the models shown in Fig. 1. Data are offset for clarity. (B) Comparisons of accuracy and precision for the resulting fits. Full fitting data are shown in Table S4. Experimental conditions are summarized in Table S4 legend.

responsible for inactivations of PSII. This model is represented by the transition probability matrix denoted VZAD in Fig. 1.

In the VZAD model, $\gamma_0 = \gamma_1 = 1 - \alpha - \beta$, $\gamma_2 = 1 - \alpha - \beta - \delta$, and $\gamma_3 = 1 - \alpha - \beta - \delta - \varepsilon$. Using STEAMM, the transition probability matrix, A, can be decomposed into

$$A = \begin{bmatrix} \alpha & \delta & \beta & \gamma_3 & 0 \\ \gamma_0 & \alpha & \delta & \beta & 0 \\ \beta & \gamma_1 & \alpha & \delta & 0 \\ \delta & \beta & \gamma_2 & \alpha & 0 \\ \varepsilon & \varepsilon & \varepsilon & \varepsilon & 1 \end{bmatrix} + \begin{bmatrix} 0 & -\delta & -\beta\varepsilon & 0 & 0 \\ 0 & 0 & \delta & -\beta\varepsilon & 0 \\ 0 & 0 & 0 & 0 & 0 \\ -\delta & 0 & 0 & 0 & 0 \\ -\varepsilon & -\varepsilon & \beta\varepsilon-\varepsilon & \beta\varepsilon & 1 \end{bmatrix} \tag{24}$$

Determination of eigenvalues for this model is slightly more challenging than the previous example due to the lower degree of symmetry apparent in the more complex perturbation matrix. However, the eigenvalues may be approximated in the first order as

$$\begin{aligned} \rho_1 &= 1 \\ \rho_2 &= 1 \\ \rho_3 &= 2(\alpha+\beta)-1+\varepsilon\ h(\alpha,\beta,\delta)/4 \\ \rho_4 &= (\alpha-\beta)-i(1-\alpha-\beta-\delta)+e(u_1+iv_1)/[2(u_2+iv_2)] \\ \rho_5 &= \overline{\rho_4} \end{aligned} \tag{25}$$

where

$$\begin{aligned} h(\alpha,\beta,\delta) = {} & [1-2\alpha+\alpha^2-8\beta+10\alpha\beta-2\alpha^2\beta+21\beta^2-12\alpha\beta^2-18\beta^3 \\ & +(1-\alpha-\beta-\delta)^2-2\beta(1-\alpha-\beta-\delta)^2-\delta+\alpha\delta+3\beta\delta+(1-\alpha-\beta-\delta)\delta \\ & -2\beta(1-\alpha-\beta-\delta)\delta][1-2\alpha+\alpha^2-6\beta+6\alpha\beta+9\beta^2+(1-\alpha-\beta-\delta) \end{aligned} \tag{26}$$

and

$$\begin{aligned} u_1 &= -2\beta^3+2\beta\alpha^2+4\alpha\beta^2-6\alpha\beta+\alpha\beta\delta+4\beta-2\beta\delta-6\beta^2+\beta^2\delta \\ u_2 &= 1+4\beta^3+\alpha^2-2\alpha+4\alpha\beta^2+2\alpha\beta-2\beta-5\beta^2+2\beta^2\delta \\ v_1 &= 2+2\alpha^2-2\beta^2-2\delta+\delta^2-4\alpha+4\alpha\beta+2\alpha\delta-4\beta+2\beta\delta \\ v_2 &= 4\beta^2+4\alpha\beta-4\beta+4\beta\delta. \end{aligned} \tag{27}$$

The phase of the VZAD model is therefore approximated as

$$\varphi_{\text{calc}} = arccos\left(\frac{Re(\lambda_4)}{|\lambda_4|}\right) \tag{28}$$

Exclusion of higher-order terms from this analysis does not significantly affect the accuracy of the model. For the data sets shown in this work, a first-order approximation of ρ_4 produces a period with relative error $\leq 0.0347\%$ compared to the numerically exact eigenvalue.

Appendix B. Supplementary data

Supplementary data to this article can be found online at http://dx.doi.org/10.1016/j.bbabio.2013.04.008.

References

[1] D.J. Vinyard, G. Ananyev, G.C. Dismukes, Photosystem II: the reaction center of oxygenic photosynthesis, Annu. Rev. Biochem. 82 (2013).

[2] G. Renger, T. Renger, Photosystem II: the machinery of photosynthetic water splitting, Photosynth. Res. 98 (2008) 53–80.

[3] F. Rappaport, M. Guergova-Kuras, P.J. Nixon, B.A. Diner, J. Lavergne, Kinetics and pathways of charge recombination in Photosystem II, Biochemistry 41 (2002) 8518–8527.

[4] P. Joliot, G. Barbieri, R. Chabaud, Un nouveau modele des centres photochimiques du systeme II, Photochem. Photobiol. 10 (1969) 309–329.

[5] B. Forbush, B. Kok, M.P. McGloin, Cooperation of charges in photosynthetic O_2 evolution—II. Damping of flash yield oscillation, deactivation, Photochem. Photobiol. 14 (1971) 307–321.

[6] B. Kok, B. Forbush, M. McGloin, Cooperation of charges in photosynthetic O_2 evolution—I. A linear four step mechanism, Photochem. Photobiol. 11 (1970) 457–475.

[7] V.P. Shinkarev, C.A. Wraight, Oxygen evolution in photosynthesis: from unicycle to bicycle, Proc. Nat. Acad. Sci. USA 90 (1993) 1834–1838.

[8] J. Jablonsky, D. Lazar, Evidence for intermediate S-states as initial phase in the process of oxygen-evolving complex oxidation, Biophys. J. 94 (2008) 2725–2736.

[9] J. Jablonsky, P. Susila, D. Lazar, Impact of dimeric organization of enzyme on its function: the case of photosynthetic water splitting, Bioinformatics 24 (2008) 2755–2759.

[10] M.-J. Delrieu, Simple explanation of the misses in the cooperation of charges in photosynthetic O_2 evolution, Photochem. Photobiol. 20 (1974) 441–454.

[11] J. Lavorel, Matrix analysis of the oxygen evolving system of photosynthesis, J. Theor. Biol. 57 (1976) 171–185.

[12] M. Gläser, C. Wolff, G. Renger, Indirect evidence for a very fast recovery kinetics of chlorophyll-aII in spinach chloroplasts, Z. Naturforsch 31c (1976) 712–721.

[13] J. van Best, P. Mathis, Kinetics of reduction of the oxidized primary electron donor of Photosystem II in spinach chloroplasts and in chlorella cells in the microsecond and nanosecond time ranges following flash excitation, Biochem. Biophys. Acta - Bioenergetics 503 (1978) 178–188.

[14] C.F. Fowler, Proton evolution from photosystem II stoichiometry and mechanistic considerations, Biochem. Biophys. Acta - Bioenergetics 462 (1977) 414–421.

[15] S. Saphon, A.R. Crofts, The H^+/e ration in chloroplasts in 2. Possible errors in its determination, Z. Naturforsch. 32 (1977) 810–816.

[16] R. Delosme, P. Joliot, Period four oscillations in chlorophyll a fluorescence, in: J. Beatty, H. Gest, J. Allen (Eds.), Govindjee, Adv. Photosynth. Respir, Springer Netherlands, 2005, pp. 379–382.

[17] W. Vredenberg, O. Prášil, A. Laisk, L. Nedbal, Govindjee, Modeling of chlorophyll a fluorescence kinetics in plant cells: derivation of a descriptive algorithm, Photosynthesis in silicoSpringer, Netherlands, 2009, pp. 125–149.

[18] G.C. Dismukes, Y. Siderer, Intermediates of a polynuclear manganese center involved in photosynthetic oxidation of water, Proc. Nat. Acad. Sci. USA 78 (1981) 274–278.

[19] B. Velthuys, Spectrophotometric studies on the S-state transitions of Photosystem II and of the interactions of its charged donor chain with lipid soluble anions, in: A. G (Ed.), Proceedings of the 5th International Congress on Photosynthesis, Balaban International Science Services, Philadelphia, 1981, pp. 75–85.

[20] H.T. Witt, E. Schlodder, K. Brettel, Ö. Saygin, Reaction sequences from light absorption to the cleavage of water in photosynthesis—routes, rates and intermediates, Ber. Bunsenges. Phys. Chem. 90 (1986) 1015–1024.

[21] M. Sivaraja, J.S. Philo, J. Lary, G.C. Dismukes, Photosynthetic oxygen evolution: changes in magnetism of the water oxidizing enzyme, J. Am. Chem. Soc. 111 (1989) 3221–3225.

[22] J. Messinger, M. Badger, T. Wydrzynski, Detection of one slowly exchanging substrate water molecule in the S_3 state of photosystem II, Proc. Nat. Acad. Sci. USA 92 (1995) 3209–3213.

[23] P. Meunier, R. Burnap, L. Sherman, Improved 5-step modeling of the Photosystem II S-state mechanism in cyanobacteria, Photosynth. Res. 47 (1996) 61–76.

[24] M.J. Delrieu, F. Rosengard, Fundamental differences between period-4 oscillations of the oxygen and fluorescence yield induced by flash excitation in inside-out thylakoids, Biochem. Biophys. Acta - Bioenergetics 892 (1987) 163–171.

[25] N.K. Packham, M. Hodges, A.L. Etienne, J.M. Briantais, Changes in the flash-induced oxygen yield pattern by thylakoid membrane phosphorylation, Photosynth. Res. 15 (1988) 221–232.

[26] V.P. Shinkarev, Oxygen evolution in photosynthesis: simple analytical solution for the Kok model, Biophys. J. 85 (2003) 435–441.

[27] V.P. Shinkarev, Flash-induced oxygen evolution in photosynthesis: simple solution for the extended S-state model that includes misses, double-hits, inactivation, and backward-transitions, Biophys. J. 88 (2005) 412–421.

[28] D.C. Lay, Linear Algebra and Its Applications, 3rd ed. Addison Wesley, Boston, 2003.

[29] D.J. Vinyard, J. Gimpel, G.M. Ananyev, M.A. Cornejo, S.S. Golden, S.P. Mayfield, G.C. Dismukes, Natural variants of Photosystem II subunit D1 tune photochemical fitness to solar intensity, J. Biol. Chem. 288 (2013) 5451–5462.

[30] G. Ananyev, G.C. Dismukes, How fast can Photosystem II split water? Kinetic performance at high and low frequencies, Photosynth. Res. 84 (2005) 355–365.

[31] G. Ananyev, T. Nguyen, C. Putnam-Evans, G.C. Dismukes, Mutagenesis of CP43-arginine-357 to serine reveals new evidence for (bi)carbonate functioning in the water oxidizing complex of Photosystem II, Photochem. Photobiol. Sci. 4 (2005) 991–998.

[32] D.R.J. Kolling, T.S. Brown, G. Ananyev, G.C. Dismukes, Photosynthetic oxygen evolution is not reversed at high oxygen pressures: mechanistic consequences for the water-oxidizing complex, Biochemistry 48 (2009) 1381–1389.

[33] K. McNeely, Y. Xu, G. Ananyev, N. Bennette, D.A. Bryant, G.C. Dismukes, *Synechococcus* sp. strain PCC 7002 *nifJ* mutant lacking pyruvate:ferredoxin oxidoreductase, Appl. Environ. Microbiol. 77 (2011) 2435–2444.

[34] A.W. Rutherford, Y. Inoue, Oscillation of delayed luminescence from PS II: recombination of S_2Q_B and S_3Q_B, FEBS Lett. 165 (1984) 163–170.

[35] A.W. Rutherford, G. Renger, H. Koike, Y. Inoue, Thermoluminescence as a probe of photosystem II. The redox and protonation states of the secondary acceptor quinone and the O_2-evolving enzyme, Biochem. Biophys. Acta - Bioenergetics 767 (1984) 548–556.

[36] G.M. Ananyev, G.C. Dismukes, Assembly of the tetra-Mn site of photosynthetic water oxidation by photoactivation: Mn stoichiometry and detection of a new intermediate, Biochemistry 35 (1996) 4102–4109.

[37] M.J.D. Powell, The BOBYQA algorithm for bound constrained optimization without derivatives, Technical Report NA2009/06, Department of Applied Mathematics and Theoretical Physics, Cambridge, England, 2009.

[38] M.J.D. Powell, A direct search optimization method that models the objective and constraint functions by linear interpolation, in: S. Gomex, J.-P. Hennart (Eds.), Advances in Optimization and Numerical Analysis, Kluwer Academic, Dordrecht, 1994, pp. 51–67.

[39] S.G. Johnson, The NLopt nonlinear-optimization package, Version 2.2.4, Massachusetts Institute of Technology, Cambridge, MA, 2008.

[40] S. Kirkpatrick, C.D. Gelatt, M.P. Vecchi, Optimization by simulated annealing, Science 220 (1983) 671–680.

[41] R.A. Horn, C.R. Johnson, Matrix Analysis, Cambridge University Press, New York, 1985.

[42] P.J. Davis, Circulant Matrices, Chelsea Publishing, New York, NY, 1994.

[43] R. Rippka, J. Waterbury, G. Cohen-Bazire, A cyanobacterium which lacks thylakoids, Arch. Microbiol. 100 (1974) 419–436.